1521-009X/46/11/1478–1486$35.00
Drug Metabolism and Disposition

https://doi.org/10.1124/dmd.118.082081
Drug Metab Dispos 46:1478–1486, November 2018

Gene-by-Environment Interaction of Bcrp$^{-/-}$ and Methionine- and Choline-Deficient Diet–Induced Nonalcoholic Steatohepatitis Alters SN-38 Disposition

Erica L. Toth, Hui Li, Anika L. Dzierlenga, John D. Clarke, Anna Vildhede, Michael Goedken, and Nathan J. Cherrington

Department of Pharmacology and Toxicology, University of Arizona, Tucson, Arizona (E.L.T., H.L., A.L.D., N.J.C.); Pharmaceutical Sciences, Washington State University, Spokane, Washington (J.D.C.); Pharmacokinetics, Dynamics, and Metabolism, Medicine Design, Pfizer Worldwide Research and Development, Groton, Connecticut (A.V.); and Research Pathology Services, Rutgers University, Newark, New Jersey (M.G.)

Received April 19, 2018; accepted August 9, 2018

ABSTRACT

Disease progression to nonalcoholic steatohepatitis (NASH) has profound effects on the expression and function of drug-metabolizing enzymes and transporters, which provide a mechanistic basis for variable drug response. Breast cancer resistance protein (BCRP), a biliary efflux transporter, exhibits increased liver mRNA expression in NASH patients and preclinical NASH models, but the impact on function is unknown. It was shown that the transport capacity of multidrug resistance protein 2 (MRP2) is decreased in NASH. SN-38, the active irinotecan metabolite, is reported to be a substrate for Bcrp, whereas SN-38 glucuronide (SN-38G) is a Mrp2 substrate. The purpose of this study was to determine the function of Bcrp in NASH through alterations in the disposition of SN-38 and SN-38G in a *Bcrp* knockout (Bcrp$^{-/-}$ KO) and methionine- and choline-deficient (MCD) model of NASH. Sprague Dawley [wild-type (WT)] rats and Bcrp$^{-/-}$ rats were fed either a methionine- and choline-sufficient (control) or MCD diet for 8 weeks to induce NASH. SN-38 (10 mg/kg) was administered i.v., and blood and bile were collected for quantification by liquid chromatography–tandem mass spectrometry. In Bcrp$^{-/-}$ rats on the MCD diet, biliary efflux of SN-38 decreased to 31.9%, and efflux of SN-38G decreased to 38.7% of control, but WT-MCD and KO-Control were unaffected. These data indicate that Bcrp is not solely responsible for SN-38 biliary efflux, but rather implicate a combined role for BCRP and MRP2. Furthermore, the disposition of SN-38 and SN-38G is altered by Bcrp$^{-/-}$ and NASH in a gene-by-environment interaction and may result in variable drug response to irinotecan therapy in polymorphic patients.

Introduction

Adverse drug reactions (ADRs) are becoming increasingly frequent, and approximately 1 in 20 hospital patients experiences an ADR in the United States (Bourgeois et al., 2010; Stausberg, 2014). Variations in drug response can occur due to a variety of factors, including alterations to drug-metabolizing enzymes and transporters. Understanding the mechanistic basis behind interindividual variability can potentially identify at-risk populations.

Many variations in drug response can be attributed to genetic polymorphisms in genes that are responsible for the absorption, distribution, metabolism, and excretion (ADME) processes that determine the pharmacokinetics of drugs. Single-nucleotide polymorphisms in *SLCO1B1* have been linked to increases in statin plasma concentrations as well as increases in statin-induced myopathy (Yee et al., 2018). Variations in multidrug resistance proteins have been known to influence therapeutic outcomes of anti-cancer treatments such as difluomotecan (Sparreboom et al., 2004) and doxorubicin (Lal et al., 2008). Genetic variations, however, are not the sole factor involved in variable response; alterations in response to disease pathogenesis may also affect ADME processes and contribute significantly to ADRs. Transient alterations in transporter function due to disease can alter drug disposition in a manner that closely resembles the loss of function due to genetic variations. These alterations create a phenotype that is incongruent with genotype, a phenomenon referred to as phenoconversion.

Nonalcoholic steatohepatitis (NASH) is the hepatic manifestation of metabolic syndrome. Disease progression to NASH presents with hepatocellular injury, inflammation, and fibrosis (Marra et al., 2008), and the prevalence of NASH is overall about 1.5% to 6.45% (Younossi et al., 2016). In addition to the histologic changes, there are also significant alterations to hepatic enzyme and transporter mRNA, protein expression, and function that are important to ADME processes, such as the ATP-binding cassette transporter (ABC) family (Hardwick et al., 2013; Dzierlenga et al., 2016). A global transcriptional study among NASH patients showed that the effect of NASH progression on transporters is a phenoconversion event; many uptake transporters are

This work was supported by the National Institutes of Health [Grants GM123643, HD062489, and ES006694].
https://doi.org/10.1124/dmd.118.082081.

ABBREVIATIONS: ABC, ATP-binding cassette; ADME, absorption, distribution, metabolism, and excretion; ADR, adverse drug reaction; BCRP, breast cancer resistance protein; KO, knockout; LC-MS/MS, liquid chromatography–tandem mass spectrometry; MCD, methionine- and choline-deficient; MRP, multidrug resistance protein; NASH, nonalcoholic steatohepatitis; PCR, polymerase chain reaction; SN-38G, SN-38 glucuronide; UGT, uridine 5′-diphospho-glucuronosyltransferase; UPLC, ultra-high performance liquid chromatography; WT, wild-type.

significantly downregulated, and efflux transporters like multidrug resistance protein (MRP)2, MRP3, and breast cancer resistance protein (BCRP) are significantly upregulated (Lake et al., 2011). Both MRP2 and BCRP are members of the ABC family and are located on the bile canaliculus of the liver, where they efflux endo- and xenobiotics. MRP3 is an ABC transporter located on the sinusoidal membrane, where it transports compounds back into the blood. Mislocalization of MRP2 during NASH significantly decreases its function (Dzierlenga et al., 2016), and alterations to the MRP2/MRP3 transport system can result in significantly altered drug disposition such as the increase in plasma retention of pemetrexed in rodent models of NASH (Dzierlenga et al., 2016). mRNA analyses of human NASH liver tissue have also shown an increase in *BCRP* expression during the disease (Hardwick et al., 2011). Alterations in BCRP function have not been explored, and it is important to understand changes to BCRP in the context of other transporters.

Irinotecan is a camptothecin-derivative chemotherapeutic that is used to treat colorectal cancers, the third leading cause of cancer death (Siegel et al., 2014). It undergoes hepatic metabolism to a variety of metabolites, only one of which, SN-38, is active. SN-38 is a known substrate of BCRP (Houghton et al., 2004; Tuy et al., 2016), and SN-38 glucuronide (SN-38G), like many glucuronides, is thought to be mainly exported through MRP2 (Kroetz, 2006). Patient response to irinotecan, however, is highly variable and carries a significant risk of life-threatening side effects (Falcone et al., 2007). Enzyme polymorphisms, such as *UGT1A1*28*, account for only a portion of this variability (Sadée and Dai, 2005). Hepatobiliary efflux of SN-38 and SN-38G facilitates the toxic effects in the intestine (Horikawa et al., 2002). Additionally, SN-38G in the intestine is converted back into SN-38 by β-glucuronidase and is then reabsorbed into systemic circulation, which is vital to irinotecan therapy as it prolongs circulation time (Hasegawa et al., 2006). Given the previous data on the effects of NASH on hepatobiliary transport of xenobiotics, it was hypothesized that functional alterations of BCRP and MRP2 during NASH would alter the disposition of SN-38 and SN-38G, potentially contributing to variable response. It was postulated that alterations to BCRP during NASH would significantly alter biliary elimination of SN-38 and lead to decreased plasma concentrations; it was similarly proposed that mislocalization of MRP2 could significantly reduce biliary elimination of its substrate, SN-38G, and lead to plasma accumulation. This study aimed to determine the effect of Bcrp polymorphic loss of function and NASH alone, and in a gene-by-environment interaction, on the disposition of SN-38 and SN-38G. The observations made through comparison of these models may provide mechanistic insight into interindividual variability and a basis for response prediction in human NASH patients.

Materials and Methods

Reagents. SN-38 and camptothecin were purchased from Sigma-Aldrich (St. Louis, MO), and SN-38G was purchased from Toronto Research Chemicals (Toronto, ON, Canada). Urethane, ultra-high performance liquid chromatography (UPLC)–grade acetonitrile, and UPLC-grade water were obtained from Sigma-Aldrich. Heparin was purchased from Alfa Aesar (Ward Hill, MA). ReadyScript cDNA synthesis kit, KiCqStart SYBR Green quantitative polymerase chain reaction (PCR) with low ROX master mix, and PCR primers for Bcrp and β-actin were obtained from Sigma-Aldrich. RNA Bee isolation reagent was obtained from Amsbio (Cambridge, MA).

Animals. Male *Bcrp* knockout (KO) and wild-type Sprague–Dawley rats of at least 8 weeks of age were purchased from Horizon Discovery (St. Louis, MO). Animals were housed in a University of Arizona Association for Assessment and Accreditation of Laboratory Animal Care–certified animal facility with a 12-hour light–dark cycle and allowed to acclimatize for at least 1 week before experiments. A methionine- and choline-deficient diet (MCD) or control diet from Dyets (Bethlehem, PA) was given ad libitum for 8 weeks when the animals were 16 weeks of age. After 8 weeks of diet, the animals underwent disposition studies. All handling, maintenance, care, and testing of the animals were in accordance with National Institutes of Health policy, and experimental protocols were approved by the University of Arizona Institutional Animal Care and Use Committee.

SN-38 and SN-38G Disposition Studies. A stock solution of 10 mg/ml SN-38 was prepared in dimethylsulfoxide. From this stock solution, a 0.8 mg/ml SN-38 co-solvent solution was prepared for injection. This solution was made by adding the SN-38 stock solution to a solution of ethanol, propylene glycol, and Tween 80, then diluting in water. The final proportion of each component was as follows: 14% ethanol, 40% propylene glycol, 3% Tween 80, 10% dimethylsulfoxide, and 33% water. No more than 5 ml/kg solution was administered.

Animals were anesthetized for cannulation surgery using an i.p. bolus dose of urethane (1 g/kg, up to 10 ml/kg in saline). To assess the disposition of SN-38 and SN-38G, cannulas were inserted into the jugular vein for drug and saline administration, carotid artery for blood collection, and bile duct for bile collection. Prior to dosing, blood was collected from the arterial cannula as a baseline. A bolus dose of 0.8 mg/kg SN-38 was then administered i.v. over a period of 90 seconds. After drug administration, blood was collected at 2, 7, 12, 20, and 40 minutes, whereas bile was collected at 0, 15, 30, and 45 minutes. Terminal liver and kidney were collected at 90 minutes. A portion of collected tissue was prepared for histologic analyses by fixing in 10% neutral-buffered formalin for 24 hours, then exchanging for 70% ethanol until embedded in paraffin by the University of Arizona Histology Service Laboratory. The remaining tissue was flash-frozen in liquid nitrogen for storage at −80°C. Blood was collected in heparin-coated microcentrifuge tubes and was spun down for 10 minutes at 10,000*g* to separate plasma from blood cells. Plasma and bile samples were also stored at −80°C.

SN-38 and SN-38G Quantification. Sample clean-up for blood and bile samples was performed using the Bond Elut 96 Plexa solid-phase extraction plates (Agilent, Santa Clara, CA), according to the manufacturer's protocol. Forty microliters plasma and 10 μl bile were used in the sample preparation process. The eluent was then evaporated to dryness and reconstituted in 120 μl mobile phase for injection onto the liquid chromatography–tandem mass spectrometry (LC-MS/MS). The tissue homogenates were made from 300 mg tissue and then cleaned up via protein precipitation in a 1:3 solution of homogenate to UPLC-grade acetonitrile. The samples were vortexed and kept on ice for 10 minutes, and then centrifuged at 13,000 rpm for 10 minutes. The supernatant was collected in a new microcentrifuge tube and evaporated to dryness. The sample was reconstituted in 120 μl mobile phase and centrifuged at 10,000 rpm for 5 minutes, and the supernatant was collected for injection onto the LC-MS/MS, as previously described (Khan et al., 2005).

The method for quantification of SN-38 and SN-38G in plasma, bile, and tissue was adapted from previously published methods (Khan et al., 2005; D'Esposito et al., 2008). The Arizona Laboratory for Emerging Contaminants at the University of Arizona provided a Waters (Milford, MA) Micromass Quattro Premier XE tandem mass spectrometer coupled to an Acquity UPLC. The mobile phase consisted of a gradient of water (solvent A) and acetonitrile (solvent B) with 0.1% formic acid at a flow rate of 0.3 ml/min through a Waters Acquity UPLC BEH C19 column (1.7 μm, 2.1 × 50 mm). The mobile phase was composed of A:B 90:10 (v:v) running to A:B 10:90 (v:v) over 1.0 to 6.0 minutes, and then returned to A:B 90:10 over 60 seconds with 2 minutes of equilibration, for a total run time of 9.0 minutes. Multiple reaction monitoring in positive mode was used to detect SN-38 at m/z 393 > 349, SN-38G at m/z 569.0 > 393.2, and camptothecin at m/z 349.1 > 305.2. The retention times for SN-38, SN-38G, and camptothecin were 3.6, 3.1, and 3.8 minutes, respectively. Recovery determination was done using four replicates, and the recovery in plasma and bile, respectively, was as follows: 76.3% and 86.8% for SN-38, 81.3% and 77.4% for SN-38G, and 80.6% and 81.8% for internal standard. The linear range of SN-38 and SN-38G in plasma was from 50 to 1000 ng/ml, and the range in bile was from 50 ng/ml to 5 μg/ml. The lower limit of quantification in plasma was found to be 15 ng/ml for SN-38 and 20 ng/ml for SN-38G; in bile, it was found to be 20 ng/ml for both SN-38 and SN-38G. Peak analysis was done in MassLynx Mass Spectrometry software (Milford, MA), and data analysis and processing were done using GraphPad Prism 5.0 (La Jolla, CA).

Quantitative Reverse Transcription-PCR. RNA was isolated from liver tissue using the RNA Bee isolation reagent. Between 200 and 300 mg tissue was added to 4 ml RNA Bee and homogenized. The manufacturer's protocol was

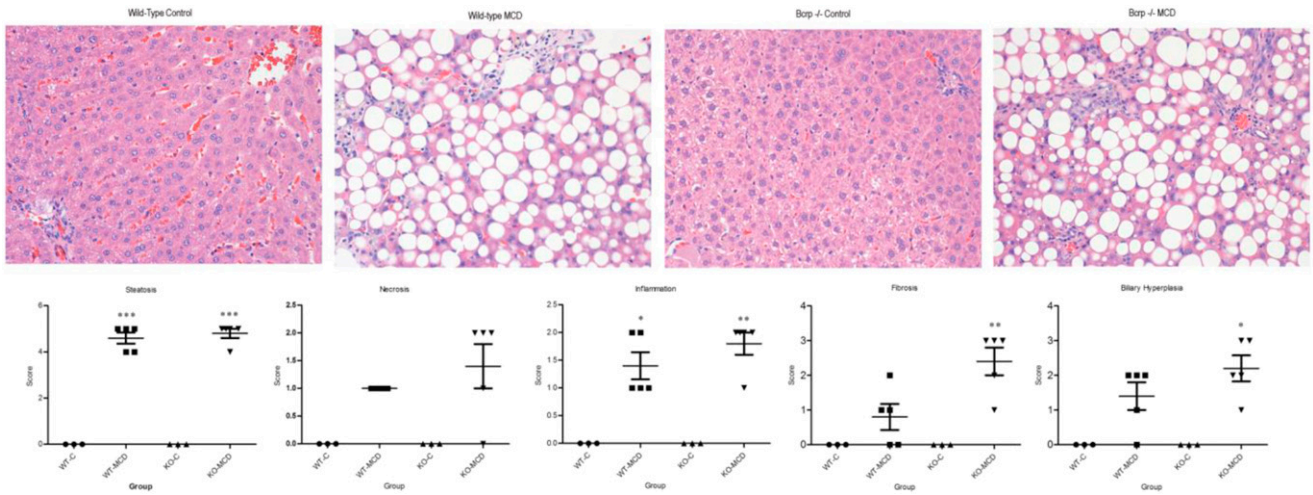

Fig. 1. Liver histopathology of control and MCD-diet rats. H&E-stained liver sections of control rats and rats fed 8 weeks of MCD diet, WT, and Bcrp KOs. Hallmark characteristics of NASH were found in MCD rats, whereas control group animals showed no signs of NASH pathology. Original magnification, 40×. Two-way analysis of variance, $*P \leq 0.05$; $**P \leq 0.01$; $***P \leq 0.001$, $n = 3$, $n = 4$ (KO-MCD).

followed, and the resulting RNA pellet was reconstituted in 250 μl DEPC (diethyl dicarbonate) water per 100 mg tissue, and then was stored at −80°C. RNA concentration was determined using a NanoDrop 2000 UV-visible spectrophotometer (Thermo Fisher Scientific, Waltham, MA). Final preparations of RNA had a 260/280 quality ratio between 1.6 and 1.9. cDNA was prepared from the isolated RNA using the ReadyScript cDNA synthesis kit from Sigma-Aldrich. Each reaction well contained 1× KiCqStart SYBR Green master mix, 100 nM forward and reverse primers, 2 μl cDNA template, and nuclease-free water up to 20 μl, run in duplicate. Reactions were run on an ABI (Waltham, MA) StepOnePlus Real Time PCR system with the standard SYBR Green PCR cycling profile. Fold change was determined using the δ-δ C_T method.

Histopathology. Paraffin-embedded liver sections were stained with H&E and then examined by a board-certified veterinary pathologist. Tissues were incidence and severity scored using an established rodent NASH system (Kleiner et al., 2005) with endpoints including steatosis, necrosis, inflammation, hyperplasia, and biliary hyperplasia. Representative digital images were acquired. Rank-order statistical methods and one-way analysis of variance were used to determine differences between groups.

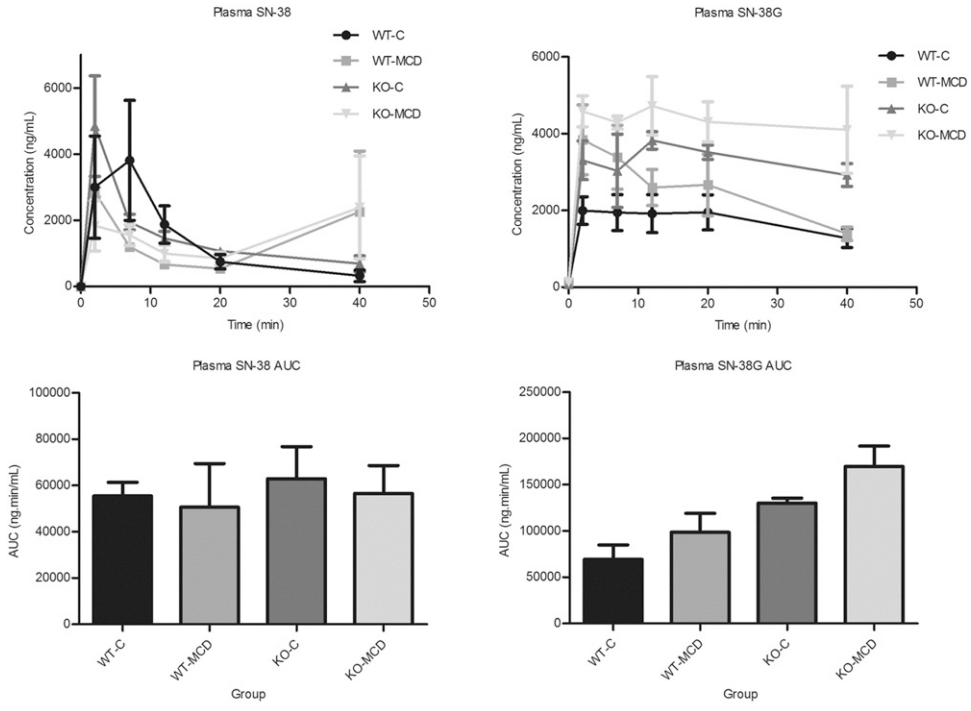

Fig. 2. Effects of MCD diet on systemic exposure of SN-38 and SN-38G. Plasma concentrations were taken over 40 minutes after i.v. infusion of 0.8 mg/kg SN-38. Graphs represent mean ± S.D., $n = 3$, $n = 4$ (KO-MCD).

2-Way ANOVA	Plasma SN-38
Interaction	0.9573
Genotype	0.6335
Disease	0.6906

2-Way ANOVA	Plasma SN-38G
Interaction	0.7741
Genotype	0.0049
Disease	0.0797

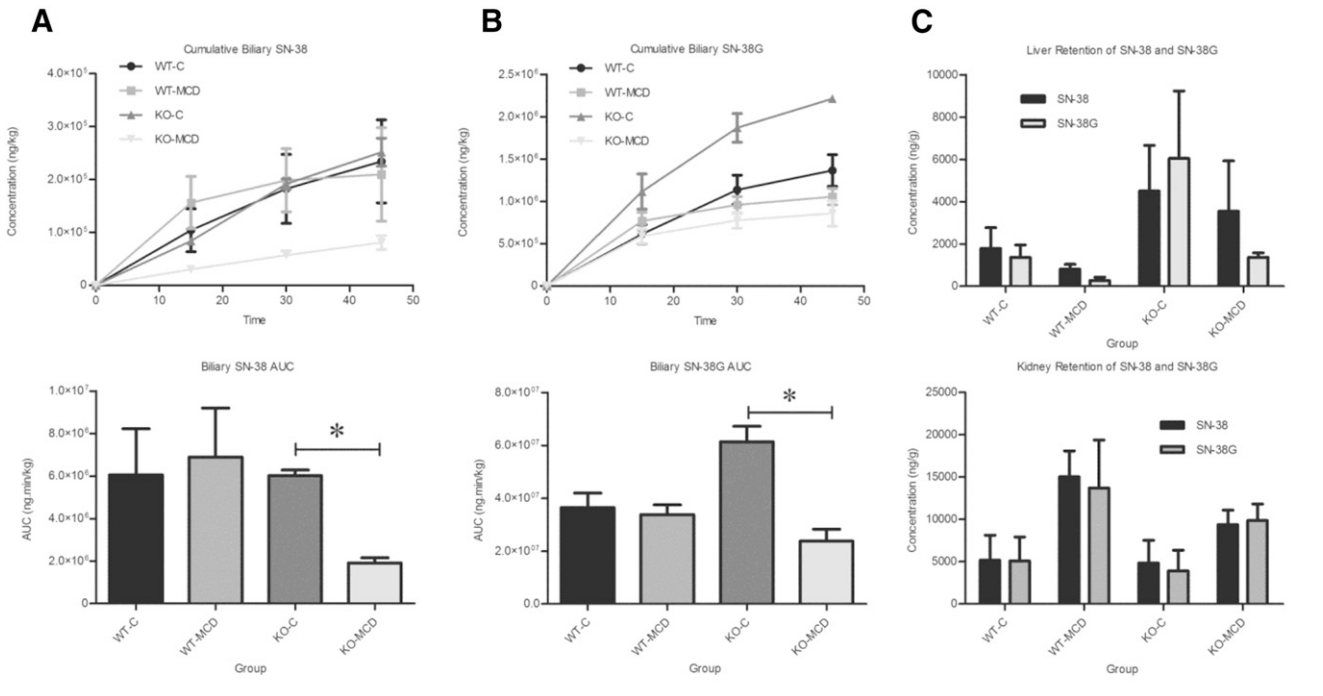

2-Way ANOVA	Bile SN-38
Interaction	0.0153
Genotype	0.0145
Disease	0.4871

2-Way ANOVA	Bile SN-38G
Interaction	0.0066
Genotype	0.1699
Disease	0.0029

2-Way ANOVA	Liver SN-38	Liver SN-38G
Interaction	0.9966	0.2602
Genotype	0.1827	0.0838
Disease	0.62	0.0847

2-Way ANOVA	Kidney SN-38	Kidney SN-38G
Interaction	0.3237	0.697
Genotype	0.2722	0.4733
Disease	0.0201	0.0582

Fig. 3. Effects of MCD diet on biliary excretion of (A) SN-38 (A) and (B) SN-38G, and (C) tissue retention of SN-38 and SN-38G. Bile concentrations were taken over 45 minutes after i.v. infusion of 0.8 mg/kg SN-38. Graphs represent mean ± S.D. Two-way analysis of variance, $*P \leq 0.05$, $n = 3$, $n = 4$ (KO-MCD).

Immunohistochemistry. Immunohistochemistry staining was performed on formalin-fixed paraffin-embedded tissue slides. The slides were deparaffinized in 100% xylene and hydrated in 100% ethanol. Antigen retrieval was performed in boiling pH 9.0 Tris-EDTA. Endogenous peroxidases were blocked using 0.3% (v/v) H_2O_2 in phosphate-buffered saline for 20 minutes. MRP2 was stained by incubating the slides overnight at 4°C with anti-MRP2 antibody (M8163; Sigma-Aldrich, St. Louis, MO), followed by the Mach 4 staining kit protocol (Biocare Medical, Pacheco, CA). Images were taken using a Leica (Wetzlar, Germany) DM4000B microscope with a DFC450 camera.

Protein Preparation. Crude membrane fractions were obtained from liver samples. Approximately 500 mg tissue was homogenized in 5 ml cold ST buffer [sucrose Tris buffer, 10 mM Tris base, and 250 mM sucrose with 1 protease inhibitor cocktail tablet (Roche, Indianapolis, IN) per 25 ml, pH 7.5]. Homogenates were centrifuged at 10,000*g* for 20 minutes to remove nuclei; the supernatant was decanted into a second set of ultracentrifuge tubes. The supernatant was spun at 100,000*g* for 60 minutes to pellet the membranes. Membrane pellets were rinsed with buffer before being resuspended in 200 μl buffer and stored at −80°C. Protein concentrations were determined by bicinchoninic acid assay (Thermo Fisher Scientific).

Immunoblotting. Immunoblotting for MRP2 and MRP3 was performed using crude membrane preparations. Membrane preparations (60 μg/lane) were separated by SDS-PAGE on 7.5% polyacrylamide gels. The proteins were transferred to polyvinylidene difluoride membranes, and then blocked with 5% nonfat dry milk in Tris-buffered saline/Tween 20 for at least 1 hour. The membranes were probed with MRP2 (M8163; Sigma-Aldrich) or MRP3 (SC-5775; Santa Cruz Biotechnology, Santa Cruz, CA) primary antibody at a dilution of 1:500 in 2.5% blocking solution. Image processing and analysis through the ImageJ software (National Institutes of Health, Bethesda, MD) determined relative protein density, and the proteins were normalized to the housekeeping protein ERK2 (SC-125; Santa Cruz Biotechnology).

Targeted Proteomic Quantitation of Bcrp Surrogate Peptide. Homogenization of liver tissues was done in a FastPrep 24 bead mill homogenizer (MP Biomedicals, Santa Ana, CA) with 1.4-mm ceramic beads. The ProteoExtract Native Membrane protein extraction kit (EMD Millipore, Billerica, MA) was used to prepare membrane fractions according to the manufacturer's protocol, and protein concentrations were subsequently determined by bicinchoninic acid assay (Pierce, Rockford, IL). Three hundred microgram aliquots of membrane protein fraction were prepared in 100 mM ammonium bicarbonate with 3.7% w/v sodium deoxycholate, and then were reduced using 6 mM dithiothreitol for 5 minutes at 95°C. The samples were alkylated with 15 mM iodoacetamide for 20 minutes at room temperature, protected from light. Matrix for calibration curves was obtained from human serum albumin processed under the same conditions. Protein digestion was performed over 24 hours at 37°C with a protein:trypsin ratio of 1:20. The reaction was quenched with 0.2% formic acid. Bcrp peptide labeled with a stable isotope was added as internal standard to each sample postdigestion, and unlabeled peptide standard was added into the matrix samples in known concentrations. The acid-precipitated sodium deoxycholate was pelleted out of the samples by centrifugation at 16,000*g* and 4°C. The supernatant was transferred to a LoBind plate (Eppendorf, Hamburg, Germany) and evaporated under nitrogen to concentrate, and then reconstituted in 0.1% formic acid for injection onto the LC-MS/MS.

Peptide quantification was performed on an API-6500 triple-quadrupole mass spectrometer operating in ESI (electrospray ionization) mode with a Shimadzu LC-30AD interface. The mobile phase consisted of solution A, 0.1% formic acid in water, and solution B, 0.1% formic acid in 90:10 acetonitrile:water, set to a flow rate of 0.2 ml/min. Ten microliters of sample was injected onto a Kinetex C18 core-shell column (1.7 μM, 100 Å, 100 × 2.1 mm), and separation occurred along the following solvent gradient: 5.5% mobile phase B for 5 minutes, linear gradient of 5.5% to 33.3% mobile phase B over 40 minutes, hold at 33.3% for 5 minutes, wash at 100% mobile phase B for 5 minutes, and then re-equilibration for

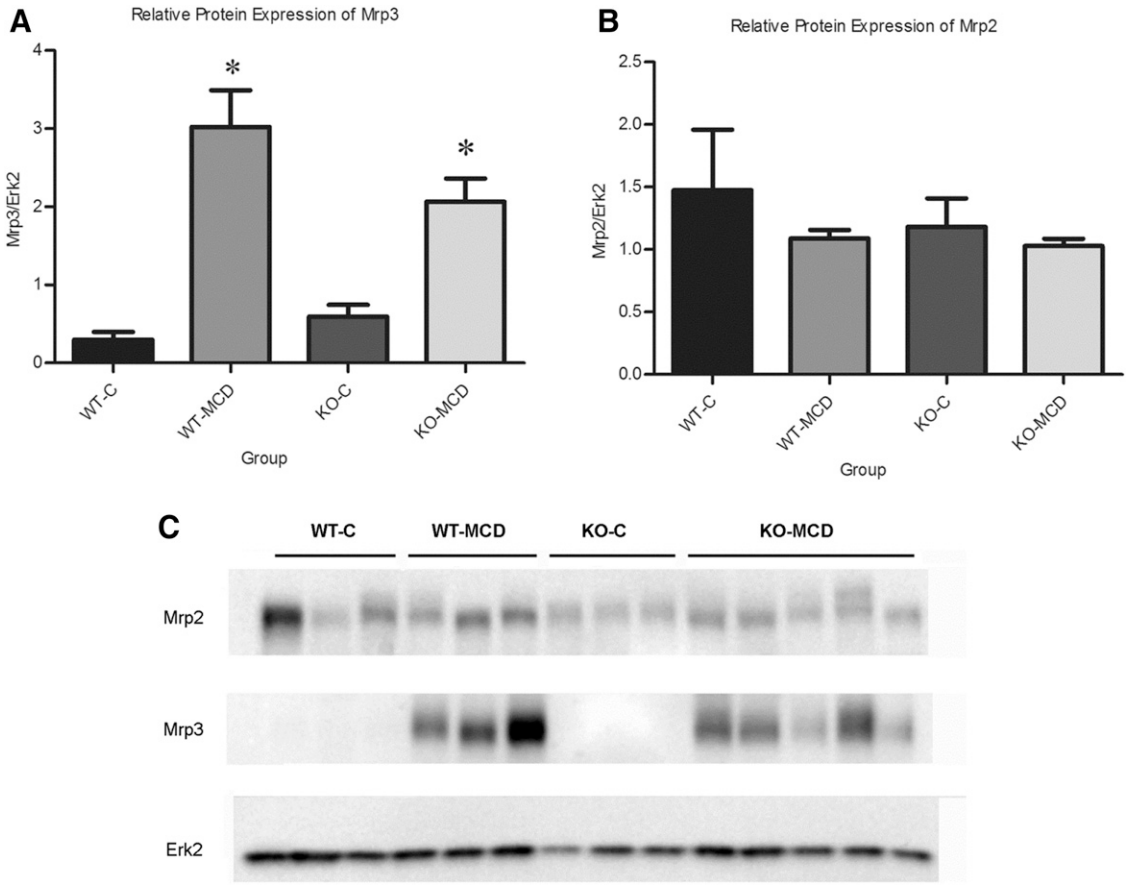

Fig. 4. Alterations of Mrp2 and Mrp3 protein expression in MCD diet. Relative protein expression of (A) Mrp2 and (B) Mrp3 between control and MCD groups. (C) Relative protein expression was determined by immunoblot analysis. Graphs represent mean ± S.D. Two-way analysis of variance, $*P \leq 0.05$, $n = 3$, $n = 4$ (KO-MCD).

4 minutes. Multiple reaction monitoring was used to detect the analyte peptide (SSLLDVLAAR) at transition 523.1 > 757.5 and the stable isotope peptide at 528.1 > 767.5. The mass spectrometer settings were as follows: 500°C source temperature, 5 kV ion spray voltage, 10 eV entrance potential, 50 V declustering potential, 25 V collision energy, and 15 V collision cell exit potential. Data were processed in Analyst 1.6.2 (SCIEX, Ontario, Canada), and the external peptide calibration curve was used to determine BCRP peptide concentration in the samples.

Statistical Analyses. All results are represented as the mean ± S.D. Two-way analysis of variance statistical analyses with Bonferroni post-test were used to compare between control and NASH animals of each genotype group. Each group consisted of $n = 3$ animals, except for KO-MCD group, which consisted of $n = 4$.

Results

Effects of MCD Diet–Induced NASH on the Disposition of SN-38 and SN-38G. H&E-stained liver sections were examined under a light microscope at 40× magnification for histologic analysis (Fig. 1). NASH hallmarks were observed in rats fed a MCD diet for 8 weeks, including steatosis, inflammation, necrosis, fibrosis, and biliary hyperplasia. This is consistent with previous observations using an established NASH scoring system and recapitulates the histologic findings in human disease (Kleiner et al., 2005; Canet et al., 2014). There was no significant interaction between the genetic KO and disease in the severity of NASH hallmarks, except for fibrosis; in KO-MCD animals, fibrosis was more severe than in KO-Control animals. The effects of NASH on SN-38 and SN-38G disposition were observed over 90 minutes. The plasma area under the curve of SN-38 and SN-38G showed no significant alterations between MCD groups and their controls (Fig. 2). Significant reductions in biliary efflux were seen for SN-38 and SN-38G between the KO-C and KO-MCD groups (Fig. 3, A and B). Biliary efflux of SN-38 in the KO-MCD group decreased to 31.9% of control (from 5.59 ± 0.102 to 1.79 ± 0.058 μg/min), and efflux of SN-38G decreased to 38.7% of control (from 49.18 ± 0.944 to 19.15 ± 2.04 μg/min).

The hepatic and renal tissue concentrations of SN-38 and SN-38G showed high variability and no statistically significant differences between the MCD groups and their controls (Fig. 3C).

Effects of MCD Diet–Induced NASH on Mrp2 and Mrp3 Protein. Relative protein concentrations of MRP2 and MRP3 and localization of MRP2 were determined by Western blotting and immunohistochemistry, respectively. Densitometric analysis was used to compare relative protein expression between groups (Fig. 4). MRP3 increased by 10-fold in the wild-type (WT)-MCD group when compared with control, and increased by 3.5-fold in the KO-MCD group when compared with control. Protein concentrations of MRP2 remained relatively unchanged between the WT-Control and WT-MCD groups and the KO-Control and KO-MCD groups (Fig. 5). Immunohistochemical staining of MRP2 revealed normal localization at the canalicular membrane in the control groups, whereas MCD groups showed pockets of internalized staining, indicating mislocalization consistent with previous observations (Dzierlenga et al., 2015, 2016).

Effects of MCD Diet–Induced NASH on Bcrp. mRNA expression of Bcrp was determined by quantitative reverse-transcription PCR, and relative protein concentration was determined by LC-MS/MS analysis of BCRP surrogate peptide (Fig. 6). *Bcrp* mRNA increased by 2-fold in the WT-MCD group when compared with its control, whereas both KO groups showed no expression. Protein expression of BCRP increased in

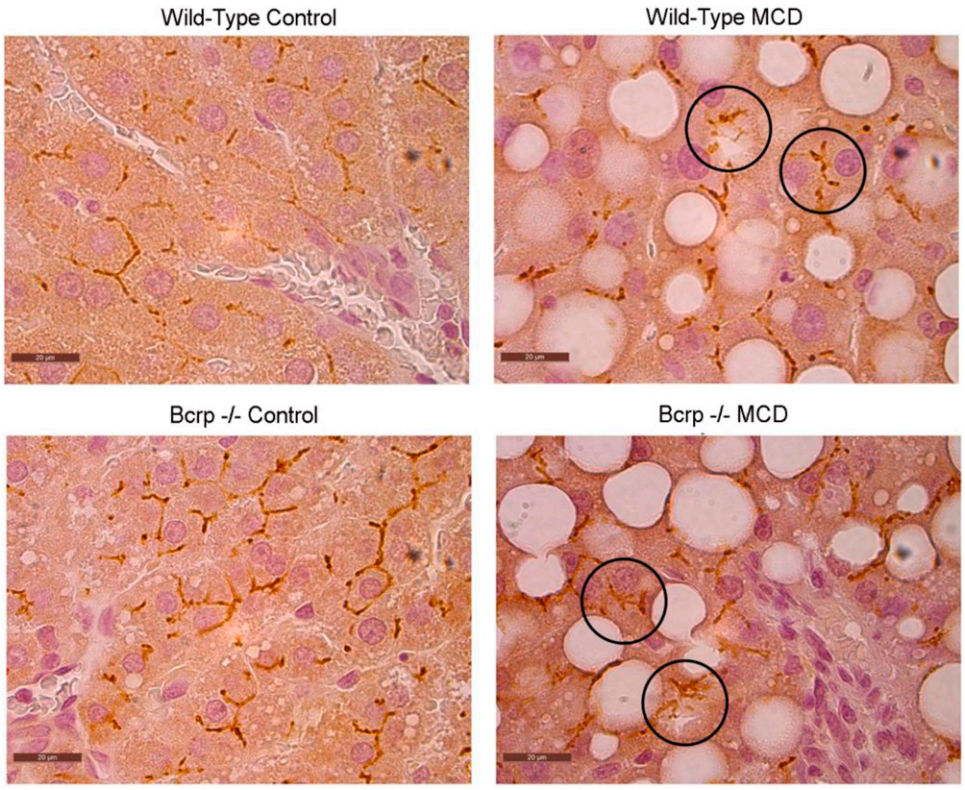

Fig. 5. Mislocalization of Mrp2 in MCD diet. Protein localization of Mrp2 was visualized by immunohistochemistry in paraffin-embedded liver tissue of controls and MCD groups. Representative images were taken at original magnification, 100×.

keeping with mRNA expression, showing a 1.6-fold increase in the MCD group when compared with controls, and no expression in the KO groups.

Discussion

The hepatobiliary disposition of SN-38 and SN-38G is mediated by BCRP and MRP2 transport, and, during NASH, alterations to BCRP function can significantly impact systemic drug exposure. It has been previously established that alterations of hepatobiliary efflux pathways can affect the distribution of xenobiotics in bile and plasma, potentially increasing patient exposure and the risk of toxicity. The MRP2/MRP3 hepatobiliary efflux pathway has been found to play a significant role in the distribution of various xenobiotics, including the chemotherapeutics pemetrexed and methotrexate, and analgesics like morphine (Hardwick et al., 2014; Dzierlenga et al., 2015, 2016; Ferslew et al., 2015). The participation of other transport proteins can also affect the distribution and toxicity of xenobiotics. Uptake transporters contribute significantly to the uptake and clearance of various drugs, including SN-38. In human patients, the hepatic uptake of ^{99m}Tc-mebrofenin, a substrate for OATP1B1 and OATP1B3, was significantly decreased in NASH due to disease-related impairment (Ali et al., 2017). *Oatp1a/1b*$^{-/-}$ mice exhibit increased SN-38 concentrations in plasma and have more pronounced neutropenia (Iusuf et al., 2014). Although hepatic uptake transporters can cause alterations in xenobiotic disposition, efflux transporters are generally considered to have the most significant impact (Köck and Brouwer, 2012). SN-38 and its metabolite SN-38G are substrates for MRP2, MRP3, and BCRP, and their disposition is significantly affected by the functional status of these transporters (Kato et al., 2002). Although it has been previously noted that SN-38 is a substrate for Bcrp and SN-38G is a substrate for MRP2 (Chu et al., 1997; Kawabata et al., 2001), our data confirm that both compounds are substrates for both transporters. The data in this work indicate that biliary efflux of SN-38 and SN-38G is unchanged either by genetic disruption of Bcrp or the NASH-related disruption of MRP2 function alone, but the combination of disease and genetic disruption significantly impedes biliary efflux.

The disposition of SN-38 and its metabolite will also be influenced by the activity of UDP-glucuronosyltransferases. Uridine 5′-diphospho-glucuronosyltransferase (UGT)1A1 is one of the major isoforms responsible for the glucuronidation of SN-38 (Etienne-Grimaldi et al., 2015), and variants of UGT1A1 have been shown to increase the risk of neutropenia in human patients taking irinotecan (Liu et al., 2014). The impact of NASH on UGT expression has been explored in previous research; in human patients, there is no change in either the mRNA or protein expression of UGT1A1 in NASH when compared with normal patients (Lake et al., 2011; Hardwick et al., 2013). Similarly, the MCD diet model of NASH had no impact on the mRNA or protein expression of UGT1A1 in rats, making it unlikely that alterations to the disposition of SN-38G would be due to the effects of the disease on this enzyme (Hardwick et al., 2012).

Uptake transporters may also have an effect on the disposition of SN-38. SN-38 is known to be transported by human OATP1B1, OATP1B3, and OATP2B1 (Kalliokoski and Niemi, 2009; Fujita et al., 2016), and rodent transporters OATP1B2, OATP2B1, and OATP1A4 (Wang et al., 2016), although other transporters of organic anions may also be involved. The MCD diet has been shown to alter the mRNA and protein expression of various hepatic uptake transporters, including rat OATP1A1, OATP1A3, OATP1B2, and OATP2B1. Decreases have been observed in the mRNA expression of *Oatp1a1*, *1a4*, *1b2*, and *2b1*, whereas protein expression of Oatp1A1, 1B2, and 2B1 decreases and 1A4 does not change (Fisher et al., 2009). Whereas mRNA and protein expression of transporters significantly impact drug disposition, the glycosylation status of these transporters will also play a role. The N-linked glycosylation of transporters has multiple functions,

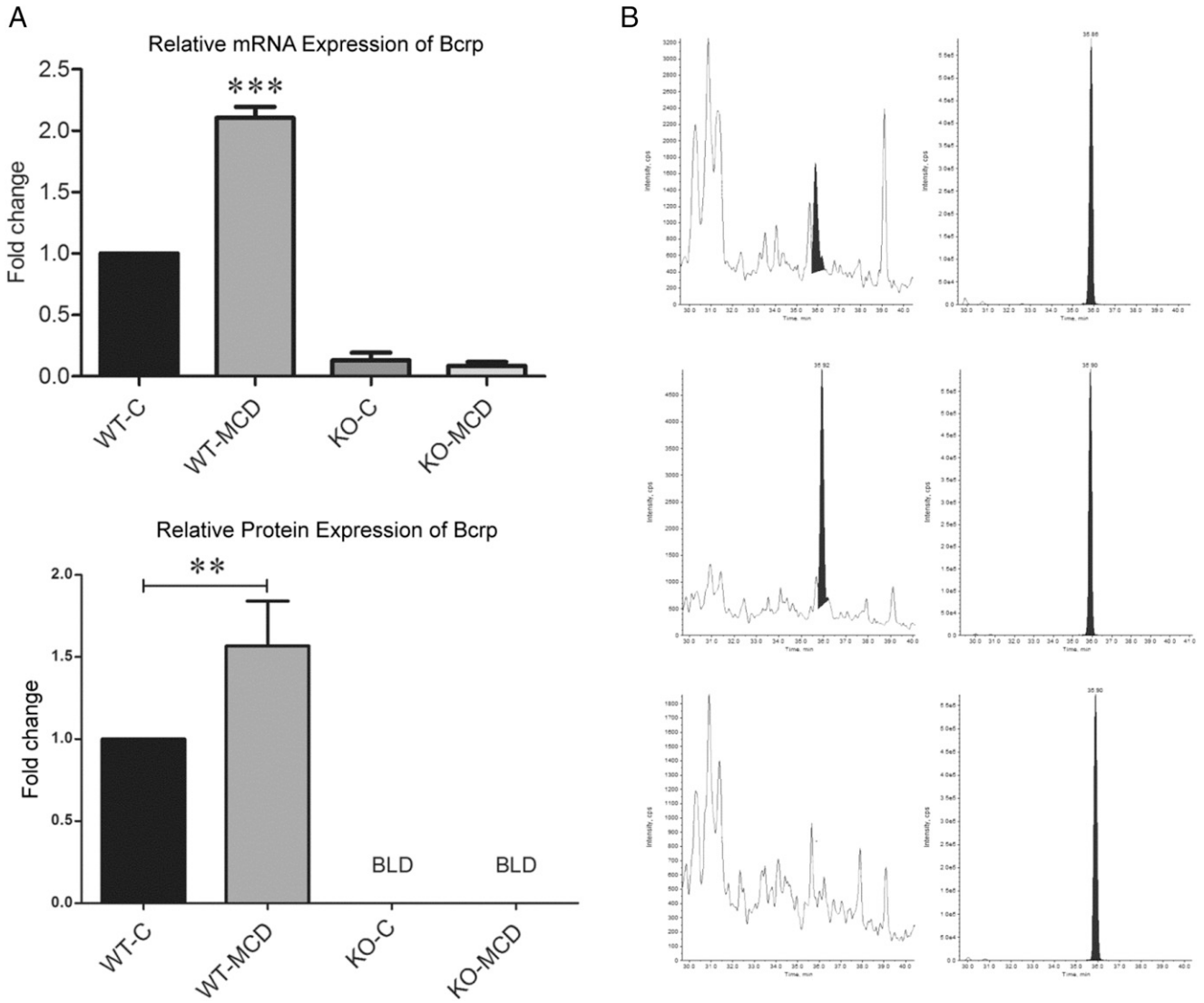

Fig. 6. Alterations of Bcrp protein and mRNA expression during MCD diet. (A) mRNA expression was determined by quantitative reverse-transcription PCR analysis, and fold change was determined using the δ-δ C_T method. Protein expression was determined by proteomic analysis using LC-MS/MS. Graphs represent mean ± S.D. Two-way analysis of variance, $^*P \leq 0.05$; $^{**}P \leq 0.01$, $^{***}P \leq 0.001$, $n = 3$, $n = 4$ (KO-MCD). (B) Representative chromatograms of WT-Control, WT-MCD, and KO groups. Left chromatogram depicts native protein concentration, and right chromatogram depicts internal standard peptide.

including protein maturation, stability, and function, and membrane-bound proteins in particular rely on proper glycosylation for protein folding and trafficking to the appropriate membrane (Urquhart et al., 2005; Tannous et al., 2015). In human NASH, it has been observed that genes involved in N-glycan synthesis are downregulated, indicating a perturbation of N-linked glycosylation. This perturbation is reflected in the increase in unglycosylated OATP1B1, OATP1B3, OATP2B1, and NTCP protein found in human NASH patients (Clarke et al., 2017). Disruption of normal glycosylation may be one mechanism by which NASH alters the function of transporter proteins.

Interindividual variability can be accounted for in some cases by genetic polymorphisms; the function of hepatic transport proteins, however, can be affected not only by genetic variation, but also by disease state. NASH has been known to cause alterations in multiple efflux transporters, including MRP2 and MRP3. There is a trend toward increased efflux transporter expression in NASH in both the human disease and rodent MCD models (Hardwick et al., 2011; Canet et al., 2014). The interactions of these disease-induced alterations with genetic polymorphisms and their functional consequences, however, have not been fully determined. Previous studies have shown gene-by-environment interactions between NASH and genetic loss of OATP transporters that affects the disposition of statins (Clarke et al., 2014). The plasma and muscle concentrations of pravastatin were synergistically increased in *Oatp1b2*$^{-/-}$ mice with NASH, indicating an increased risk for statin toxicity. Myopathy is the major adverse effect of statin therapy, and it is known to be dose dependent and related to plasma concentrations; this synergistic increase between the genotype and disease indicates a potential at-risk patient group of those with OATP1B1 polymorphisms and NASH. We found that NASH causes an alteration to the normal hepatobiliary efflux of SN-38 and SN-38G by perturbing the MRP2/MRP3 efflux pathway through mislocalization of MRP2 and increased expression of MRP3. Compensation, however, occurs in the form of upregulated BCRP, restoring sufficient biliary efflux and leading to no significant alteration in SN-38 or SN-38G elimination in the MCD rodent model. There is a significant gene-by-environment effect observed with the addition of a genetic *Bcrp* KO to the MCD diet, whereby removal of the compensatory BCRP upregulation results in a sharp decrease in biliary elimination of both parent compound and

metabolite. There was no significant increase in plasma area under the curve over the observed time points, although alteration to the plasma retention may only be observable at points after the final 40-minute time point. Similarly, there was no statistically significant difference in SN-38 or SN-38G retention in kidney or liver tissues when compared with controls. We can therefore conclude that Bcrp plays a role in the disposition of SN-38 and SN-38G along with MRP2 and MRP3, and that its function as a compensatory transporter is of increased importance in NASH. As BCRP can compensate for the loss of other transporter function during NASH, disrupting its function can restrict the biliary excretion of SN-38 and SN-38G. Systemic retention of SN-38 may increase the risk of toxicity. It has been previously seen that decreased SN-38/SN-38G ratios in plasma are a predictor of the severity of neutropenia in irinotecan therapy, although not all irinotecan toxicity could be accounted for by UGT activity (Iyer et al., 2002; Hirose et al., 2012). Diminished efflux of SN-38G may also decrease the therapeutic efficacy of irinotecan by preventing the intestinal conversion of SN-38G to SN-38 and enterohepatic recycling.

These findings provide a mechanistic basis for variable response to irinotecan therapy and identify potential risk in vulnerable populations. NASH has only recently been identified as a factor in drug disposition and ADRs, and, due to the invasive liver biopsy required for definitive diagnosis, susceptible patients may not be readily identified. Additionally, genetic variants of BCRP are relatively common, and the C421A variant can be found in 39% of Japanese and 30% of Caucasian populations, producing a transporter with a nonfunctional ATP-binding domain (Imai et al., 2002; Kobayashi et al., 2005). A less abundant variant, G34A, exists in 18% of Japanese populations, 6% of African–American populations, and 3% of Caucasian populations (Imai et al., 2002; Noguchi et al., 2009). Genetic variation in BCRP has also been shown to cause alterations to the pharmacokinetics and pharmacodynamics of drugs on its own (Zhang et al., 2006; Mizuno et al., 2012), and the combination of genetic polymorphisms and disease could potentially compound these changes, as demonstrated in this work with SN-38. With the increasing prevalence of NASH, the importance of phenoconversion in patients who also have genetic polymorphisms is significant. These data provide a possible mechanistic basis for previously unidentified causes of variability and toxicity to BCRP substrates in NASH patients.

Acknowledgments

We thank Dr. Leif Abrell for assistance with LC-MS/MS method development.

Authorship Contributions

Participated in research design: Toth, Li, Dzierlenga, Clarke, Cherrington.

Conducted experiments: Toth, Li, Dzierlenga, Clarke, Vildhede.

Performed data analysis: Toth, Vildhede, Goedken.

Wrote or contributed to the writing of the manuscript: Toth, Li, Clarke, Dzierlenga, Vildhede, Goedken, Cherrington.

References

Ali I, Slizgi JR, Kaullen JD, Ivanovic M, Niemi M, Stewart PW, Barritt AS, IV, and Brouwer KLR (2017) Transporter-mediated alterations in patients with NASH increase systemic and hepatic exposure to an OATP and MRP2 substrate. *Clin Pharmacol Ther* DOI: 10.1002/cpt.997 [published ahead of print].

Bourgeois FT, Shannon MW, Valim C, and Mandl KD (2010) Adverse drug events in the outpatient setting: an 11-year national analysis. *Pharmacoepidemiol Drug Saf* **19**:901–910.

Canet MJ, Hardwick RN, Lake AD, Dzierlenga AL, Clarke JD, and Cherrington NJ (2014) Modeling human nonalcoholic steatohepatitis-associated changes in drug transporter expression using experimental rodent models. *Drug Metab Dispos* **42**:586–595.

Chu XY, Kato Y, Niinuma K, Sudo KI, Hakusui H, and Sugiyama Y (1997) Multispecific organic anion transporter is responsible for the biliary excretion of the camptothecin derivative irinotecan and its metabolites in rats. *J Pharmacol Exp Ther* **281**:304–314.

Clarke JD, Hardwick RN, Lake AD, Lickteig AJ, Goedken MJ, Klaassen CD, and Cherrington NJ (2014) Synergistic interaction between genetics and disease on pravastatin disposition. *J Hepatol* **61**:139–147.

Clarke JD, Novak P, Lake AD, Hardwick RN, and Cherrington NJ (2017) Impaired N-linked glycosylation of uptake and efflux transporters in human non-alcoholic fatty liver disease. *Liver Int* **37**:1074–1081.

D'Esposito F, Tattam BN, Ramzan I, and Murray M (2008) A liquid chromatography/electrospray ionization mass spectrometry (LC-MS/MS) assay for the determination of irinotecan (CPT-11) and its two major metabolites in human liver microsomal incubations and human plasma samples. *J Chromatogr B Analyt Technol Biomed Life Sci* **875**:522–530.

Dzierlenga AL, Clarke JD, Hargraves TL, Ainslie GR, Vanderah TW, Paine MF, and Cherrington NJ (2015) Mechanistic basis of altered morphine disposition in nonalcoholic steatohepatitis. *J Pharmacol Exp Ther* **352**:462–470.

Dzierlenga AL, Clarke JD, Klein DM, Anumol T, Snyder SA, Li H, and Cherrington NJ (2016) Biliary elimination of pemetrexed is dependent on Mrp2 in rats: potential mechanism of variable response in nonalcoholic steatohepatitis. *J Pharmacol Exp Ther* **358**:246–253.

Etienne-Grimaldi MC, Boyer JC, Thomas F, Quaranta S, Picard N, Loriot MA, Narjoz C, Poncet D, Gagnieu MC, Ged C, et al.; Collective work by Groupe de Pharmacologie Clinique Oncologique (GPCO-Unicancer); French Réseau National de Pharmacogénétique Hospitalière (RNPGx) (2015) UGT1A1 genotype and irinotecan therapy: general review and implementation in routine practice. *Fundam Clin Pharmacol* **29**:219–237.

Falcone A, Ricci S, Brunetti I, Pfanner E, Allegrini G, Barbara C, Crinò L, Benedetti G, Evangelista W, Fanchini L, et al.; Gruppo Oncologico Nord Ovest (2007) Phase III trial of infusional fluorouracil, leucovorin, oxaliplatin, and irinotecan (FOLFOXIRI) compared with infusional fluorouracil, leucovorin, and irinotecan (FOLFIRI) as first-line treatment for metastatic colorectal cancer: the Gruppo Oncologico Nord Ovest. *J Clin Oncol* **25**:1670–1676.

Ferslew BC, Johnston CK, Tsakalozou E, Bridges AS, Paine MF, Jia W, Stewart PW, Barritt AS, IV, and Brouwer KL (2015) Altered morphine glucuronide and bile acid disposition in patients with nonalcoholic steatohepatitis. *Clin Pharmacol Ther* **97**:419–427.

Fisher CD, Lickteig AJ, Augustine LM, Oude Elferink RPJ, Besselsen DG, Erickson RP, and Cherrington NJ (2009) Experimental non-alcoholic fatty liver disease results in decreased hepatic uptake transporter expression and function in rats. *Eur J Pharmacol* **613**:119–127.

Fujita D, Saito Y, Nakanishi T, and Tamai I (2016) Organic anion transporting polypeptide (OATP)2B1 contributes to gastrointestinal toxicity of anticancer drug SN-38, active metabolite of CPT-11. *Drug Metab Dispos* **44**:1–7.

Hardwick RN, Clarke JD, Lake AD, Canet MJ, Anumol T, Street SM, Merrell MD, Goedken MJ, Snyder SA, and Cherrington NJ (2014) Increased susceptibility to methotrexate-induced toxicity in nonalcoholic steatohepatitis. *Toxicol Sci* **142**:45–55.

Hardwick RN, Ferreira DW, More VR, Lake AD, Lu Z, Manautou JE, Slitt AL, and Cherrington NJ (2013) Altered UDP-glucuronosyltransferase and sulfotransferase expression and function during progressive stages of human nonalcoholic fatty liver disease. *Drug Metab Dispos* **41**:554–561.

Hardwick RN, Fisher CD, Canet MJ, Scheffer GL, and Cherrington NJ (2011) Variations in ATP-binding cassette transporter regulation during the progression of human nonalcoholic fatty liver disease. *Drug Metab Dispos* **39**:2395–2402.

Hardwick RN, Fisher CD, Street SM, Canet MJ, and Cherrington NJ (2012) Molecular mechanism of altered ezetimibe disposition in nonalcoholic steatohepatitis. *Drug Metab Dispos* **40**:450–460.

Hasegawa Y, Ando Y, Ando M, Hashimoto N, Imaizumi K, and Shimokata K (2006) Pharmacogenetic approach for cancer treatment-tailored medicine in practice. *Ann N Y Acad Sci* **1086**: 223–232.

Hirose K, Kozu C, Yamashita K, Maruo E, Kitamura M, Hasegawa J, Omoda K, Murakami T, and Maeda Y (2012) Correlation between plasma concentration ratios of SN-38 glucuronide and SN-38 and neutropenia induction in patients with colorectal cancer and wild-type UGT1A1 gene. *Oncol Lett* **3**:694–698.

Horikawa M, Kato Y, and Sugiyama Y (2002) Reduced gastrointestinal toxicity following inhibition of the biliary excretion of irinotecan and its metabolites by probenecid in rats. *Pharm Res* **19**:1345–1353.

Houghton PJ, Germain GS, Harwood FC, Schuetz JD, Stewart CF, Buchdunger E, and Traxler P (2004) Imatinib mesylate is a potent inhibitor of the ABCG2 (BCRP) transporter and reverses resistance to topotecan and SN-38 in vitro. *Cancer Res* **64**:2333–2337.

Imai Y, Nakane M, Kage K, Tsukahara S, Ishikawa E, Tsuruo T, Miki Y, and Sugimoto Y (2002) C421A polymorphism in the human breast cancer resistance protein gene is associated with low expression of Q141K protein and low-level drug resistance. *Mol Cancer Ther* **1**:611–616.

Iusuf D, Ludwig M, Elbatsh A, van Esch A, van de Steeg E, Wagenaar E, van der Valk M, Lin F, van Tellingen O, and Schinkel AH (2014) OATP1A/1B transporters affect irinotecan and SN-38 pharmacokinetics and carboxylesterase expression in knockout and humanized transgenic mice. *Mol Cancer Ther* **13**:492–503.

Iyer L, Das S, Janisch L, Wen M, Ramírez J, Karrison T, Fleming GF, Vokes EE, Schilsky RL, and Ratain MJ (2002) UGT1A1*28 polymorphism as a determinant of irinotecan disposition and toxicity. *Pharmacogenomics J* **2**:43–47.

Kalliokoski A and Niemi M (2009) Impact of OATP transporters on pharmacokinetics. *Br J Pharmacol* **158**:693–705.

Kato Y, Suzuki H, and Sugiyama Y (2002) Toxicological implications of hepatobiliary transporters. *Toxicology* **181–182**:287–290.

Kawabata S, Oka M, Shiozawa K, Tsukamoto K, Nakatomi K, Soda H, Fukuda M, Ikegami Y, Sugahara K, Yamada Y, et al. (2001) Breast cancer resistance protein directly confers SN-38 resistance of lung cancer cells. *Biochem Biophys Res Commun* **280**:1216–1223.

Khan S, Ahmad A, Guo W, Wang YF, Abu-Qare A, and Ahmad I (2005) A simple and sensitive LC/MS/MS assay for 7-ethyl-10-hydroxycamptothecin (SN-38) in mouse plasma and tissues: application to pharmacokinetic study of liposome entrapped SN-38 (LE-SN38). *J Pharm Biomed Anal* **37**:135–142.

Kleiner DE, Brunt EM, Van Natta M, Behling C, Contos MJ, Cummings OW, Ferrell LD, Liu YC, Torbenson MS, Unalp-Arida A, et al.; Nonalcoholic Steatohepatitis Clinical Research Network (2005) Design and validation of a histological scoring system for nonalcoholic fatty liver disease. *Hepatology* **41**:1313–1321.

Kobayashi D, Ieiri I, Hirota T, Takane H, Maegawa S, Kigawa J, Suzuki H, Nanba E, Oshimura M, Terakawa N, et al. (2005) Functional assessment of ABCG2 (BCRP) gene polymorphisms to protein expression in human placenta. *Drug Metab Dispos* **33**:94–101.

Köck K and Brouwer KLR (2012) A perspective on efflux transport proteins in the liver. *Clin Pharmacol Ther* **92**:599–612.

Kroetz DL (2006) Role for drug transporters beyond tumor resistance: hepatic functional imaging and genotyping of multidrug resistance transporters for the prediction of irinotecan toxicity. *J Clin Oncol* **24**:4225–4227.

Lake AD, Novak P, Fisher CD, Jackson JP, Hardwick RN, Billheimer DD, Klimecki WT, and Cherrington NJ (2011) Analysis of global and absorption, distribution, metabolism, and

elimination gene expression in the progressive stages of human nonalcoholic fatty liver disease. *Drug Metab Dispos* **39**:1954–1960.
Lal S, Wong ZW, Sandanaraj E, Xiang X, Ang PCS, Lee EJD, and Chowbay B (2008) Influence of ABCB1 and ABCG2 polymorphisms on doxorubicin disposition in Asian breast cancer patients. *Cancer Sci* **99**:816–823.
Liu X, Cheng D, Kuang Q, Liu G, and Xu W (2014) Association of UGT1A1*28 polymorphisms with irinotecan-induced toxicities in colorectal cancer: a meta-analysis in Caucasians. *Pharmacogenomics J* **14**:120–129.
Marra F, Gastaldelli A, Svegliati Baroni G, Tell G, and Tiribelli C (2008) Molecular basis and mechanisms of progression of non-alcoholic steatohepatitis. *Trends Mol Med* **14**:72–81.
Mizuno T, Fukudo M, Terada T, Kamba T, Nakamura E, Ogawa O, Inui K, and Katsura T (2012) Impact of genetic variation in breast cancer resistance protein (BCRP/ABCG2) on sunitinib pharmacokinetics. *Drug Metab Pharmacokinet* **27**:631–639.
Noguchi K, Katayama K, Mitsuhashi J, and Sugimoto Y (2009) Functions of the breast cancer resistance protein (BCRP/ABCG2) in chemotherapy. *Adv Drug Deliv Rev* **61**:26–33.
Sadée W and Dai Z (2005) Pharmacogenetics/genomics and personalized medicine. *Hum Mol Genet* **14 Spec No. 2**:R207–R214.
Siegel R, Desantis C, and Jemal A (2014) Colorectal cancer statistics, 2014. *CA Cancer J Clin* **64**:104–117.
Sparreboom A, Gelderblom H, Marsh S, Ahluwalia R, Obach R, Principe P, Twelves C, Verweij J, and McLeod HL (2004) Diflomotecan pharmacokinetics in relation to ABCG2 421C>A genotype. *Clin Pharmacol Ther* **76**:38–44.
Stausberg J (2014) International prevalence of adverse drug events in hospitals: an analysis of routine data from England, Germany, and the USA. *BMC Health Serv Res* **14**:125.
Tannous A, Pisoni GB, Hebert DN, and Molinari M (2015) N-linked sugar-regulated protein folding and quality control in the ER. *Semin Cell Dev Biol* **41**:79–89.
Tuy HD, Shiomi H, Mukaisho KI, Naka S, Shimizu T, Sonoda H, Mekata E, Endo Y, Kurumi Y, Sugihara H, et al. (2016) ABCG2 expression in colorectal adenocarcinomas may predict resistance to irinotecan. *Oncol Lett* **12**:2752–2760.
Urquhart P, Pang S, and Hooper NM (2005) N-glycans as apical targeting signals in polarized epithelial cells. *Biochem Soc Symp* **72**:39–45.
Wang X, Rao Z, Qin H, Zhang G, Ma Y, Jin Y, Han M, Shi A, Wang Y, and Wu X (2016) Effect of hesperidin on the pharmacokinetics of CPT-11 and its active metabolite SN-38 by regulating hepatic Mrp2 in rats. *Biopharm Drug Dispos* **37**:421–432.
Yee SW, Brackman DJ, Ennis EA, Sugiyama Y, Kamdem LK, Blanchard R, Galetin A, Zhang L, and Giacomini KM (2018) Influence of transporter polymorphisms on drug disposition and response: a perspective from the International Transporter Consortium. *Clin Pharmacol Ther* DOI: 10.1002/cpt.1098 [published ahead of print].
Younossi ZM, Koenig AB, Abdelatif D, Fazel Y, Henry L, and Wymer M (2016) Global epidemiology of nonalcoholic fatty liver disease-Meta-analytic assessment of prevalence, incidence, and outcomes. *Hepatology* **64**:73–84.
Zhang W, Yu BN, He YJ, Fan L, Li Q, Liu ZQ, Wang A, Liu YL, Tan ZR, Fen-Jiang, et al. (2006) Role of BCRP 421C>A polymorphism on rosuvastatin pharmacokinetics in healthy Chinese males. *Clin Chim Acta* **373**:99–103.

Address correspondence to: Dr. Nathan J. Cherrington, Department of Pharmacology and Toxicology, University of Arizona, 1703 East Mabel Street, Tucson, AZ 85721. E-mail: cherrington@pharmacy.arizona.edu